Neuron 50, 603–616, May 18, 2006 ©2006 Elsevier Inc. DOI 10.1016/j.neuron.2006.04.019

The $GABA_{B1b}$ Isoform Mediates Long-Lasting Inhibition of Dendritic Ca^{2+} Spikes in Layer 5 Somatosensory Pyramidal Neurons

Enrique Pérez-Garci,[1] Martin Gassmann,[2] Bernhard Bettler,[2] and Matthew E. Larkum[1,*]
[1] Institute of Physiology
University of Bern
Bühlplatz 5
CH-3012 Bern
Switzerland
[2] Pharmazentrum
Department of Clinical-Biological Sciences
Institute of Physiology
University of Basel
CH-4056 Basel
Switzerland

Summary

The apical tuft of layer 5 pyramidal neurons is innervated by a large number of inhibitory inputs with unknown functions. Here, we studied the functional consequences and underlying molecular mechanisms of apical inhibition on dendritic spike activity. Extracellular stimulation of layer 1, during blockade of glutamatergic transmission, inhibited the dendritic Ca^{2+} spike for up to 400 ms. Activation of metabotropic $GABA_B$ receptors was responsible for a gradual and long-lasting inhibitory effect, whereas $GABA_A$ receptors mediated a short-lasting (~150 ms) inhibition. Our results suggest that the mechanism underlying the $GABA_B$ inhibition of Ca^{2+} spikes involves direct blockade of dendritic Ca^{2+} channels. By using knockout mice for the two predominant $GABA_{B1}$ isoforms, $GABA_{B1a}$ and $GABA_{B1b}$, we showed that postsynaptic inhibition of Ca^{2+} spikes is mediated by $GABA_{B1b}$, whereas presynaptic inhibition of GABA release is mediated by $GABA_{B1a}$. We conclude that the molecular subtypes of $GABA_B$ receptors play strategically different physiological roles in neocortical neurons.

Introduction

Neocortical pyramidal neurons receive most of their inhibition (up to 80%) at their dendritic arbor (Beaulieu and Somogyi, 1990; Somogyi et al., 1998). Several classes of interneurons are located in the supragranular layers including L1, some of which are thought to form local synaptic connections with the tufts of pyramidal neurons at distances of up to 1 mm or more from the spike initiation zone in the axon (Chu et al., 2003; DeFelipe and Jones, 1988; Derer and Derer, 1990;Gonchar and Burkhalter, 1997, 1999; Hestrin and Armstrong, 1996; Radnikow et al., 2002; Somogyi et al., 1998; Zhu et al., 2004). Inputs to this region of the cell have a negligible effect on the membrane potential (V_m) in the soma and initial segment of the axon because of the huge attenuation of subthreshold signals propagating along the apical dendrite (Stuart and Spruston, 1998). Why then should inhibitory inputs selectively target the distal apical dendrite? One possibility is that they control the generation of Na^+/Ca^{2+} action potentials (for brevity referred to from this point as calcium spikes) (Buzsaki et al., 1996; Kim et al., 1995; Larkum et al., 1999b; Miles et al., 1996) in the apical tuft (Amitai et al., 1993; Schiller et al., 1997), rather than directly influencing action potential (AP) generation in the initial segment of the axon (Stuart et al., 1997). However, inhibition of dendritic Ca^{2+} spikes is still poorly understood.

A number of observations lend importance to dendritic inhibition: (1) upper cortical layers, in particular layer 1, are characterized by an extensive plexus of inhibitory axons (de Blas et al., 1988; Houser et al., 1983) that confer a major source of inhibition, whose disruption translates into hyperexcitability (Shlosberg et al., 2003); (2) excitatory cortical feedback projections to L1 (Cauller et al., 1998; Felleman and Van Essen, 1991; Rockland and Pandya, 1979) not only contact other pyramidal neurons (Rockland and Pandya, 1979) but also L1 calretinin-positive and L2/3 parvalbumin-positive interneurons (Gonchar and Burkhalter, 1999; Gonchar and Burkhalter, 2003); (3) Ca^{2+} spikes are very susceptible to local inhibitory inputs, as a single AP from one interneuron in L2/3 contacting a L5 pyramidal neuron have been shown to abolish dendritic Ca^{2+} spikes without affecting the generation or back propagation of axonally initiated Na^+ APs (Larkum et al., 1999b).

At the molecular level, the inhibitory amino acid γ-aminobutyric acid (GABA) inhibits L5 pyramidal neurons via ionotropic $GABA_A$ and metabotropic $GABA_B$ receptors, both of which are expressed on the apical dendrite (Costa et al., 2002; Fritschy et al., 1998; Gonchar et al., 2001; López-Bendito et al., 2002). Inhibitory responses mediated by each receptor type are characterized by their different time courses, but it is unclear how they affect the dynamics of Ca^{2+} spike blockade. Activation of $GABA_A$ receptors induces a relatively fast hyperpolarizing response (tens of milliseconds) largely mediated by a Cl^- conductance, although their direct effects on the membrane can be depolarizing in pyramidal neurons (Gulledge and Stuart, 2003). In addition, $GABA_A$ receptors mediate shunting inhibition, which may be more significant under some circumstances (Staley and Mody, 1992; Williams, 2005). $GABA_B$ receptors activate inwardly rectifying (GIRK or Kir3) K^+ channels via a G protein membrane-delimited pathway (for a review see Bettler et al. [2004]), inducing a slow inhibitory postsynaptic potential lasting hundreds of milliseconds (decay times of 100 to 500 ms) (Benardo, 1994; Gähwiler and Brown, 1985; Newberry and Nicoll, 1984; Shao and Burkhalter, 1999; Tamas et al., 2003). $GABA_B$ can also lead to more complex effects on postsynaptic excitability by inhibiting Ca^{2+} conductances (Bettler et al., 2004; Campbell et al., 1993; Mintz and Bean, 1993; Scholz and Miller, 1991); for example, it has been shown that $GABA_B$ receptors can inhibit dendritic Ca^{2+} currents in isolated dendritic segments of hippocampal neurons (Kavalali et al., 1997).

$GABA_B$ receptors are heterodimers consisting of two distinct subunits. The $GABA_{B1}$ subunit contains the

*Correspondence: larkum@pyl.unibe.ch

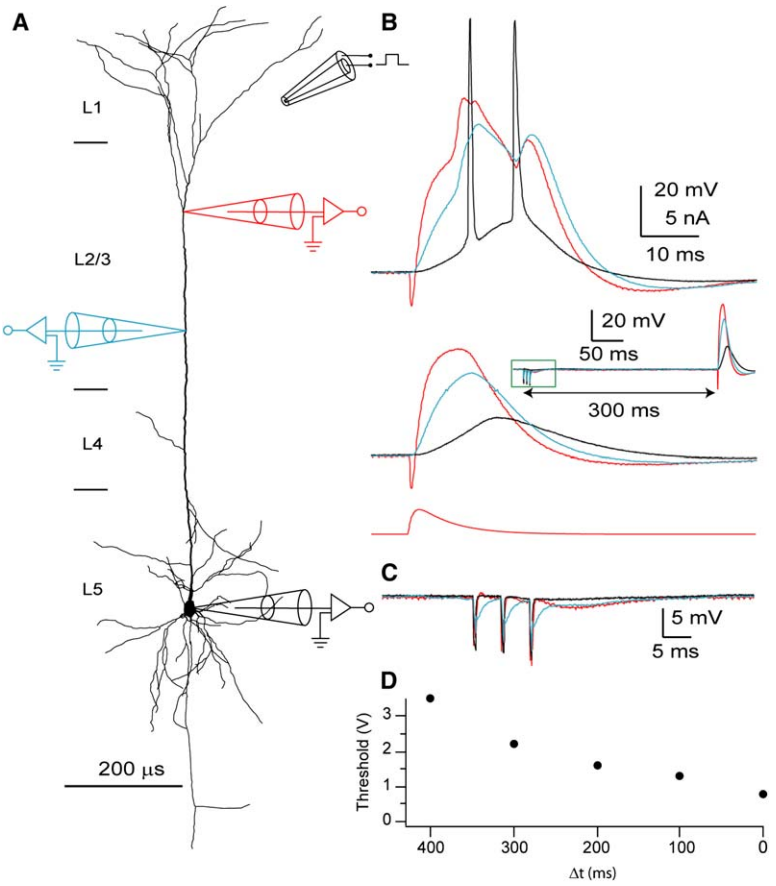

Figure 1. Activation of Distal Inhibitory Inputs Induces a Long-Lasting Inhibition of Dendritic Ca^{2+} Spikes in Rats

(A) Reconstruction of a biocytin-filled L5 pyramidal neuron from a rat showing the sites of three simultaneous recordings (red, 720 μm from soma; blue, 500 μm from soma; black, somatic) and a stimulation electrode situated in L1.

(B) Top, a dendritic Ca^{2+} spike was evoked by injecting an EPSP-shaped current wave form (double exponential shape: $f[t] = [1 - e^{-t/\tau 1}]e^{-t/\tau 2}$; in which $\tau_1 = 1$ ms and $\tau_2 = 6$ ms; time to peak: 2 ms) via the most distal pipette (red trace, bottom). Dendritic spikes propagated forward to the soma where they evoked a burst of APs (black sweep). Middle, the same dendritic current injection did not evoke a Ca^{2+} spike when three extracellular stimuli at 200 Hz were applied to L1 in the presence of CNQX (10 μM) and APV (50 μM), 300 ms before dendritic stimulation (inset). Colors of the traces correspond to pipettes shown in (A).

(C) Magnified sweeps showing the IPSP framed by the green box in the inset of (B).

(D) The minimal extracellular stimulus strength required to block the dendritic Ca^{2+} spike as a function of the time delay between dendritic and L1 stimulation.

ligand binding pocket, whereas the $GABA_{B2}$ subunit is responsible for translocation of the heterodimer from the endoplasmatic reticulum to the membrane. Two variants of the $GABA_{B1}$ subunit have been cloned, $GABA_{B1a}$ and $GABA_{B1b}$. A pre- versus and postsynaptic localization for each isoform has been proposed but because of the lack of selective ligands was never directly demonstrated (Bettler et al., 2004).

Here, we studied the effect of inhibition on dendritic Ca^{2+} spikes by extracellular stimulation of L1. We examined the duration of the inhibitory effect after pharmacological blockade of $GABA_A$ and $GABA_B$ receptors in both wild-type (wt) as well as in mice lacking either the $GABA_{B1a}$ or the $GABA_{B1b}$ isoform. Furthermore, we examined the postsynaptic effect of $GABA_B$ activation on dendritic isolated Ca^{2+} currents in the region where Ca^{2+} spikes are generated.

Results

Inhibition of Dendritic Ca^{2+} Spikes

We first examined the effect of distal inhibition on dendritic Ca^{2+} spikes (Figure 1). The Ca^{2+} spikes were evoked by direct dendritic current injection into the distal apical dendrite of L5 pyramidal neurons (Figures 1A and 1B) from the somatosensory cortex of adult rats (P28–P56). Inhibition was evoked (Figure 1B, middle) by extracellularly stimulating the upper layers of the cortex (3 pulses at 200 Hz were used to evoke a compound $GABA_A/GABA_B$ IPSP; see Figure S1 in the Supplemental Data available with this article online) (Kim et al., 1997; Scanziani, 2000) in the presence of glutamatergic antagonists (10 μM CNQX and 50 μM APV, n = 40). Extracellular stimulus strength was chosen to be near the threshold for blocking Ca^{2+} spikes. The inhibition of dendritic Ca^{2+} spikes lasted for up to 450 ms (Figure 1B, inset, and Figure 1D). The effect became gradually weaker as the delay between the extracellular stimulus and the Ca^{2+} spike increased, which was evident from the fact that the stimulus strength for blocking the Ca^{2+} spike increased (Figure 1D). Even for longer delays, the threshold stimulus strength needed for blocking dendritic Ca^{2+} spikes was relatively small and produced a small and short IPSP (Figure 1C) (~40 ms duration and ~2 mV hyperpolarization; average duration 137 ± 115 ms, average amplitude −2.4 ± 2.5 mV, n = 20). The fact that such a short IPSP was able to block Ca^{2+} spikes for 300 ms or more suggests that mechanisms in addition to simple membrane hyperpolarization or shunt were involved.

Our aim was to unravel the mechanisms underlying this form of dendritic inhibition. The long time scale of this inhibition suggested that $GABA_B$ receptor activation was involved. To examine this possibility, we used pharmacological and genetic tools, which required using a robust method to evoke and block dendritic Ca^{2+} firing. Direct dendritic current injection was not the ideal method for investigating the mechanisms of this inhibition because (1) it introduced variability because of the location of the dendritic electrode relative to the dendritic initiation zone, (2) activation of Ca^{2+} channels required a variable amount of current injection from cell

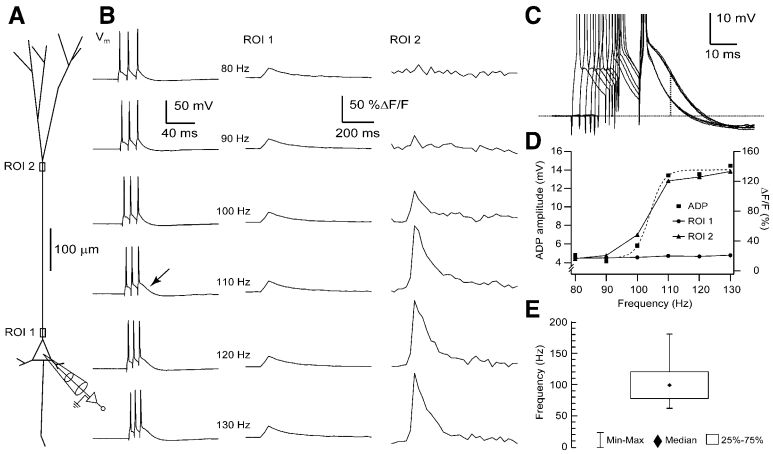

Figure 2. L5 Pyramidal Neocortical Neurons from Wild-Type Mice Exhibit Firing-Frequency-Dependent Afterdepolarization Indicating Dendritic Activity

(A) Experimental protocol showing the somatic pipette that contained the Ca^{2+} indicator OGB-1 (100 μM), allowing simultaneous monitoring of Ca^{2+} fluorescence transients (ΔF/F) at different regions of interest (ROI 1 and ROI 2).

(B) First column, firing responses of the L5 pyramidal cell to a train of three suprathreshold (1.5–2.0 nA) square current pulses (2 ms duration) injected near the soma. The second and third columns show the Ca^{2+} transients recorded at ROI 1 and ROI 2, respectively. Somatic firing frequency was varied (80 to 130 Hz) and the amplitude of the ADP after the last AP measured for each frequency. An increase in the amplitude of the ADP (arrow) corresponded to a large change in Ca^{2+} fluorescence in the distal dendrite (ROI 2) but not at soma (ROI 1).

(C) The six sweeps shown in the first column of (B) superimposed and aligned to the last AP in each train. The amplitude of the ADP was measured at the time indicated with the doted line relative to resting V_m.

(D) Amplitudes of the ADP (■) and ΔF/F (proximal ●; distal ▲) as function of the train frequency. Note the similarity between distal ΔF/F and ADP amplitudes. ADP values were fit with a sigmoidal function (dashed curve). The critical frequency was defined as the frequency at half amplitude.

(E) Distribution of the critical frequencies for all the neurons recorded (n = 48).

to cell, and (3) dendritic recordings were susceptible to changes in access resistance over the long periods of time necessary for pharmacological manipulations. To overcome these problems, we chose the "critical frequency" (CF) paradigm (Larkum et al., 1999a) to evoke dendritic Ca^{2+} activity. To take advantage of genetically manipulated mice that selectively express the $GABA_{B1a}$ and $GABA_{B1b}$ subunit isoforms (Vigot et al., 2006), we first needed to show that the CF paradigm works similarly in this species to rats (Figure 2).

As with rats (Larkum et al., 1999a), L5 cortical pyramidal neurons in mice exhibit dendritic Ca^{2+} activity after a train of 3 or 4 APs at high frequencies (~100 Hz). Somatic APs were evoked by 2 ms suprathreshold (1.5–2.0 nA) square current pulses injected at the soma (Figure 2A), in a series of frequencies in steps of 10 Hz (Figure 2B, first column). Above a specific frequency (104.7 ± 5.5 Hz; n = 48; Table 1), referred to here as the "critical frequency" (CF), a prominent afterdepolarizing potential (ADP) (8.0 ± 0.4 mV; Table 1) was observed after the last AP (Figure 2B, first column, indicated by the arrow).

In addition to the electrophysiological recordings at the soma, Ca^{2+} fluorescence measurements were performed after loading the neuron with the Ca^{2+} indicator OGB-1 (100 μM) via the somatic recording pipette. Two regions of interest (ROIs) were monitored along the axis of the apical dendrite, one proximal to the soma (~20–100 μm) (Figure 2A, ROI 1) and another at a distal region where Ca^{2+} spikes are normally evoked (>500 μm) (Figure 2A, ROI 2) (Larkum and Zhu, 2002). A large increase in the Ca^{2+} fluorescence transient (ΔF/F) was observed at the distal location ROI 2, at the CF (Figure 2B), but not at the proximal location, ROI 1. The increase in amplitude of the ADP observed at the somatic recording (Figure 2B, first column) corresponded to the increase in distal ΔF/F (Figure 2B, ROI 2).

The amplitude of the ADP was measured for each frequency (Figure 2C) and plotted as a function of the firing frequency (Figure 2D, squares). A sigmoidal fit was performed in order to quantify the CF value of each cell (Figure 2D, dashed curve), which was defined as the frequency at half amplitude of the fitted curve. ΔF/F amplitudes recorded at both ROIs (Figure 2D, right axis, triangles and circles) were plotted on the same graph to show the correspondence between $\Delta[Ca^{2+}]_i$ in the distal dendrite and the change in the ADP. The ADP reflects the dendritic Ca^{2+} activity propagating toward the soma (Larkum et al., 1999a). The similarity between distal $\Delta[Ca^{2+}]_i$ and the somatic ADP at all frequencies indicates that the ADP can be used as a substitute readout for determining the CF.

The average CF of L5 pyramidal neurons in mice was 104.7 ± 5.5 Hz (median 99 Hz; n = 48; Table 1), which was similar to the CF in rats (98 ± 6 Hz) (Larkum et al., 1999a), and the distribution was also similarly skewed toward higher frequencies (range 61–183 Hz) (Figure 2E) (see also Larkum et al. [1999a]). From this point onward, we show only the results for mice, although similar data were also obtained in rats (except for experiments in which knockout mice were used).

Table 1. Electrophysiological Properties of L5 Pyramidal Neurons in Wild-Type and $GABA_{B1}$-Isoform Knockout Mice

	RMP (mV)	R_N (MΩ)	Rheobase (pA)	CF (Hz)	ADP (mV)
Wild-type (n = 48)	65.7 ± 0.6	37.0 ± 1.4	339.6 ± 15.7	104.7 ± 5.5	8.0 ± 0.4
$GABA_{B1a}^{-/-}$ (n = 14)	64.5 ± 0.6	41.7 ± 3.4	300.0 ± 25.7	104.2 ± 10.4	7.1 ± 0.5
$GABA_{B1b}^{-/-}$ (n = 17)	63.9 ± 0.5	38.8 ± 3.4	323.5 ± 20.2	115.5 ± 9.0	7.3 ± 0.8

RMP, resting membrane potential; R_N, input resistance; Rheobase, threshold current for AP; CF, critical frequencies; ADP, afterdepolarizing potential at a supracritical frequency.

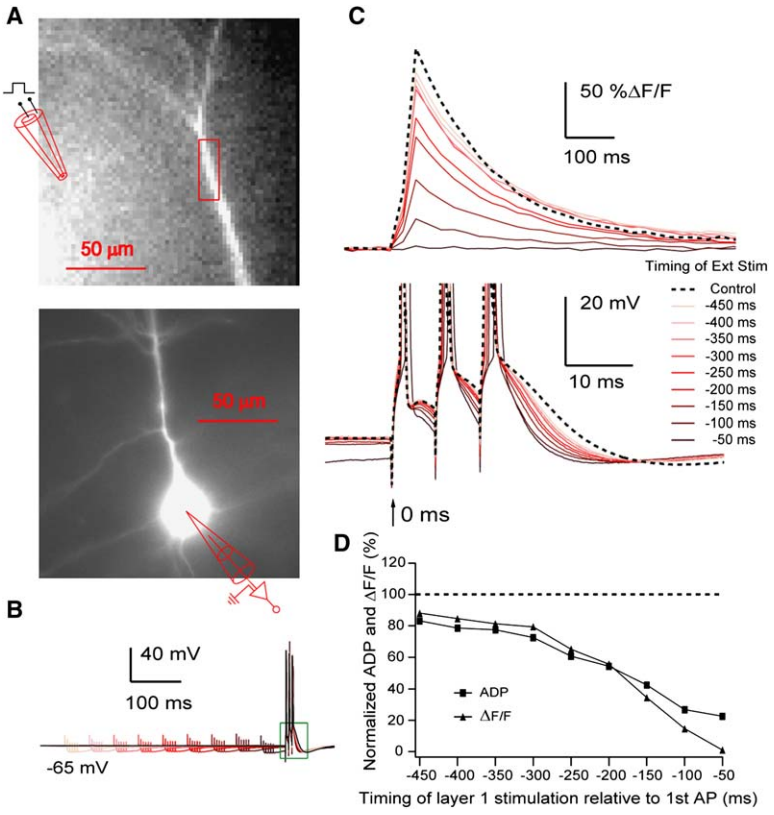

Figure 3. Activation of Distal Inhibitory Inputs Induces a Long-Lasting Blockade of Dendritic Ca^{2+} Fluorescence and ADP

(A) Experimental arrangement. Somatic whole-cell voltage recordings were made with a pipette containing OGB-1 (100 μM; bottom) while monitoring ΔF/F at a distal ROI on the apical dendrite, 600 μm from soma (red box, top). An extracellular bipolar electrode was set in L1 around 100 μm from the vertical axis of the apical dendrite.

(B) Electrical recordings from the soma while evoking a train of three APs at 150 Hz with current injection (CF was 88 Hz in this neuron). A compound IPSP was concurrently evoked by stimulating L1 (five pulses at 200 Hz) in the presence of CNQX (10 μM) and APV (50 μM). The time of the extracellular L1 stimulation varied from −450 to −50 ms before the AP train in steps of 50 ms, relative to the first somatic AP.

(C) Gradual blockade of distal Ca^{2+} transients (top) and ADPs recorded at the soma (bottom; magnified sweeps from the green box in [B]) were observed as the compound IPSP approached the first AP. Dashed curves indicate the control values in the absence of L1 stimulation.

(D) Inhibition curves. Areas underneath ADPs (■) and ΔF/F amplitudes (▲), normalized to the values observed in the absence of L1 stimulation (dashed line), plotted as a function of the delay between the L1 extracellular stimuli and the first AP.

We next examined the effect of time-varying extracellularly evoked inhibition on dendritic Ca^{2+} activity with the CF paradigm (Figure 3). After determining the CF for each cell, we used a fixed supra-CF train of somatic APs (Figure 3B) for the rest of the experiment while measuring Ca^{2+} fluorescence transients in the distal apical dendrite (Figure 3A, ROI, red box, >500 μm from the soma, Figure 3C, top) and ADPs at the soma (Figure 3C, bottom). After establishing the control values (dashed lines, Figure 3C), glutamatergic transmission was blocked by application of CNQX (10 μM) and APV (50 μM). The CF, ΔF/F, and ADP values remained unaltered in the presence of these drugs. Under these conditions, we could evoke a compound IPSP (Figure 3B) in the pyramidal neuron with a train of 3 to 5 extracellular stimuli at 200 Hz to L1 (these parameters were chosen to achieve stable activation of $GABA_B$ receptors) (see Figure S1) (Kim et al., 1997; Scanziani, 2000). This was done with a bipolar electrode placed 100–200 μm from the vertical axis of the apical dendrite (Figure 3A, top). The intensity of the L1 stimulus was adjusted until no further decrease in distal fluorescence could be detected for the shortest stimulation interval, 50 ms (Figure 3C, darkest solid sweep; see also Figure S1). At this stimulus level, the amplitudes of somatic APs were never affected by L1 stimulation. Note, the recordings in Figure 3C were single sweeps indicating that partial (rather than all-or-none) block of $\Delta[Ca^{2+}]_i$ occurred.

The extracellular stimulus train was then evoked at times 450–50 ms in steps of 50 ms before the somatic AP train. The shorter the interval between stimulation and AP train, the more the dendritic Ca^{2+} transients and the ADP amplitudes were attenuated (Figure 3C). Figure 3D depicts the time course of the inhibition ("inhibition curve") of the ΔF/F amplitudes and areas underneath the ADP, normalized to the values obtained in absence of extracellular stimulation. Note the similarity between the inhibition curves of both parameters, indicating that ADP on its own constitutes a reliable measure of distal dendritic activity. Using either method, we demonstrated that the inhibitory effect of L1 stimulation lasted on average up to 400 ms (n = 11; Figures 3–5). This also shows that the CF paradigm for investigating distal inhibition in mice was equivalent to the protocol shown in Figure 1 in which direct dendritic current was used to evoke Ca^{2+} spikes in rats. This is most likely due to the fact that both methods activate the same ionic currents, which are then blocked by inhibition.

One possible explanation for the action of inhibition might be a shunt of the back-propagating APs (Tsubokawa and Ross, 1996) rather than direct blockade of dendritic Ca^{2+} spikes. However, to fully rule out this possibility, we repeated the experiments with dendritic recordings (Figure 4A; n = 4). As in Figure 3, AP amplitudes at the soma were not affected by the L1 stimulus at any time, but there was a gradual block of the ADP (Figure 4C, bottom). The dendritic patch recording revealed a similar gradual decrease in the area under the last AP in the train for times from 400 to 50 ms before the somatic AP train (Figure 4C, top). However, when the L1 stimulus was exactly coincident with the somatic AP train (0 ms, blue traces) the second and third APs were severely shunted (second AP amplitude reduced to 7 mV versus 35 mV for the control amplitude, 80% reduction). This completely abolished the summation of back-propagating APs in the dendrite. If the L1 stimulus

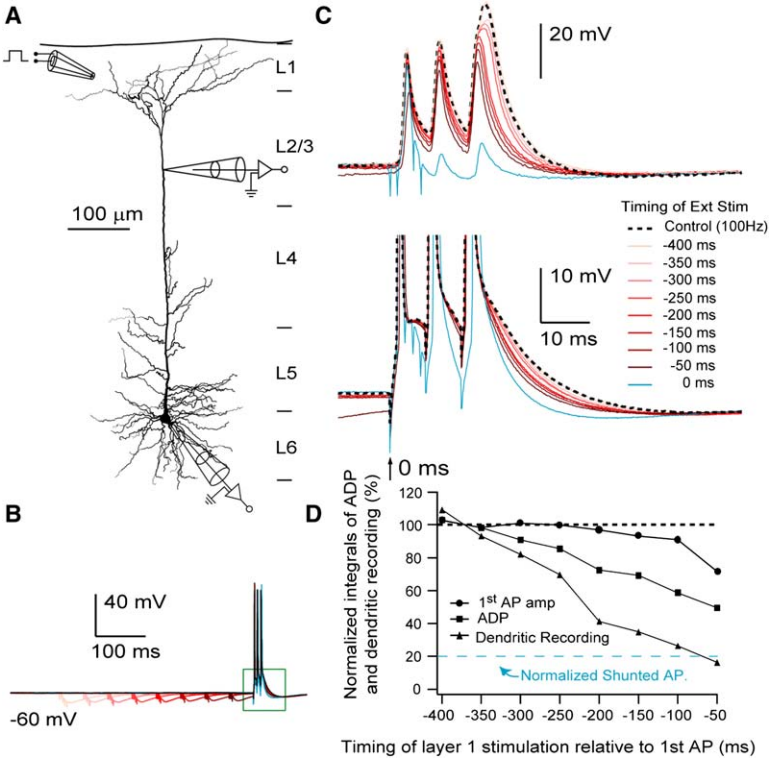

Figure 4. L1 Extracellular Stimulus Did Not Shunt Back-Propagating APs

(A) Experimental configuration. Simultaneous somatic and distal dendritic (~480 μm) whole-cell recordings. An extracellular bipolar electrode was placed in L1 around 150 μm from the vertical axis of the apical dendrite.

(B) Same as Figure 3B. Here, the somatic APs were evoked at 140 Hz (CF = 105 Hz).

(C) Single-voltage recordings showing a gradual blockade of dendritic activity (top) and ADP in the somatic recording (bottom; magnified sweeps from the green box in [B]) was observed as the compound IPSP approached the first AP of the train. Dashed curves indicate the control values in the absence of L1 stimulation and blue traces, shunted APs when the stimulus was coincident with the AP train (0 ms).

(D) Inhibition curves comparing the area underneath the somatic ADP (■) and last dendritic AP (▲) normalized to the values observed in the absence of L1 stimulation (short-dashed line). The amplitude of the first back-propagated AP normalized to the first back-propagated AP value in the absence of L1 stimulation is also plotted against stimulus time (●). The percentage amplitude of a fully shunted AP with L1 stimulus at t = 0 is indicated with a blue dashed line (20%).

strength was reduced, the back-propagating APs were not shunted even at 0 ms, whereas the dendritic Ca^{2+} activity continued to be blocked (data not shown), indicating that the effect of distal inhibition was much stronger on Ca^{2+} activity than on AP propagation. The gradual block of the somatic ADP (Figure 4D, squares) and the area under third dendritic AP (Figure 4D, triangles) are shown as a function of stimulus timing. The amplitude of the first dendritic AP in the train (Figure 4D, circles) was not substantially changed at most times indicating that shunt of the back-propagating AP did not underlie the gradual block of dendritic Ca^{2+} activity. Using dV/dt instead of amplitude gave exactly the same result (data not shown). Because our main interest was the effect of inhibition on dendritic Ca^{2+} activity, we restricted the times of stimulation to >50 ms to avoid effects because of shunting of the back-propagating APs for the rest of the study.

Receptors Underlying the Inhibition of Dendritic Ca^{2+} Spikes

We then sought to investigate the contribution of $GABA_A$ and $GABA_B$ receptors to the long-lasting inhibitory effects. After establishing the inhibition curves while blocking glutamatergic transmission (Figures 5B–5E, red curves), we repeated the stimulation protocol with sequential pharmacological blockade of $GABA_B$ and $GABA_A$ receptors (Figure 5A, middle and right columns, respectively). Pharmacological disinhibition of the dendritic Ca^{2+} activity was detected with dendritic Ca^{2+} fluorescence (Figure 5A, top row) and the ADP amplitude (Figure 5A, bottom row). The $GABA_B$ receptor antagonist CGP52432 (1 μM; Figure 5A, middle column) abolished the long-lasting inhibitory component (Figures 5B–5E, blue curves). Under these conditions, inhibition was only effective for up to 150 ms before the first somatic AP (Figures 5B–5E). Blockade of $GABA_A$ receptors with the antagonist gabazine (3 μM), in the constant presence of CGP52432, removed the remaining inhibitory component (Figures 5B–5E, green curves). These pharmacological properties were consistent across all neurons tested (n = 11, Figures 5C and 5E). $GABA_B$ receptor activity accounted for the inhibition at most times, indicating an important role for this receptor in dendritic inhibition.

Activation of $GABA_B$ receptors is known to activate Ba^{2+}-sensitive K^+ currents (Takigawa and Alzheimer, 1999) and inhibit Ca^{2+} currents (Kavalali et al., 1997) in isolated dendrites of pyramidal neurons. Which action of $GABA_B$ receptors account for the inhibition of dendritic Ca^{2+} spikes? The duration of the compound IPSP evoked by L1 stimulation was shorter than the duration of the blocking effect on Ca^{2+} spikes evoked in the dendrite either by direct dendritic current injection (see Figure 1) or by using supra-critical frequency AP trains (dendritic IPSP duration: 210 ± 11 ms, n = 4; somatic IPSP duration: 182 ± 16, n = 11). This implies that activation of GIRK conductance cannot fully explain the time course of inhibition of dendritic Ca^{2+} spikes.

We looked more closely at the underlying mechanism of $GABA_B$-induced block of dendritic Ca^{2+} spikes by puffing baclofen locally onto the dendritic initiation zone (Figure 6A). Puffing 50 μM baclofen onto the dendrite caused a local hyperpolarization at a nearby dendritic recording site of 37 ± 9 s (n = 3) in duration but not at the somatic recording site (Figure 6B). We estimated that the axial spread of the puffed substance was around 100 μm (see Experimental Procedures). 200 μM Ba^{2+} reduced the duration (39% ± 3%) and amplitude (63% ± 3%) of this hyperpolarization (n = 3; Figures 6B and 6D). On the other hand, blockade of

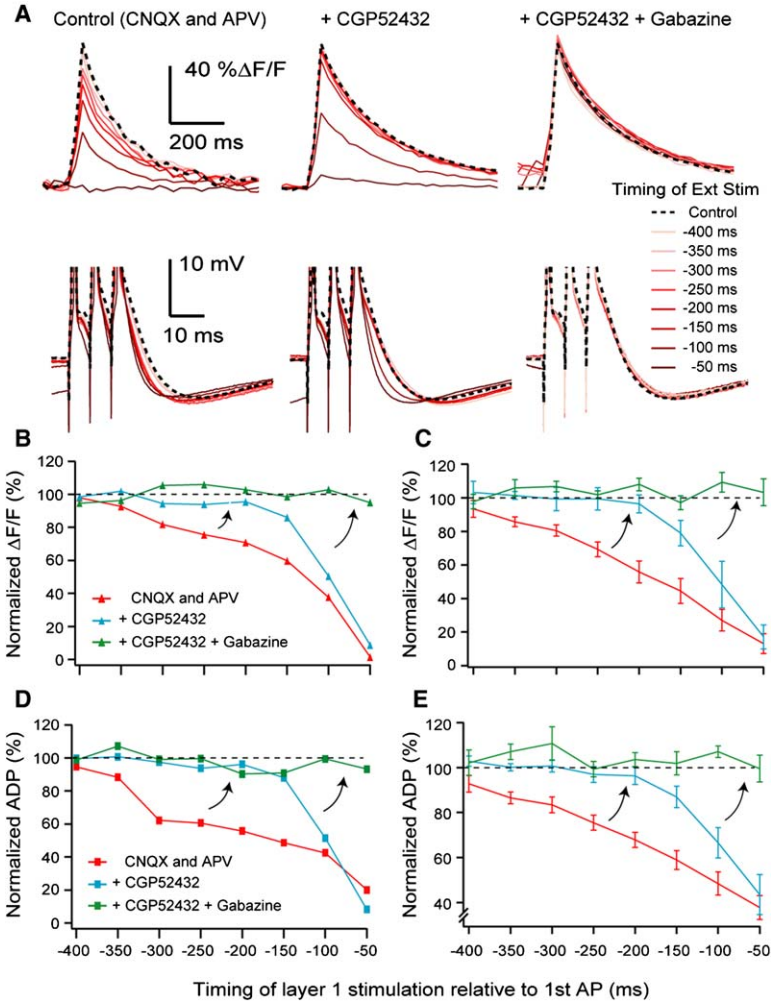

Figure 5. Activation of $GABA_B$ Receptors Is Responsible for the Long-Lasting Inhibition of Distal Ca^{2+}Activity

(A) Left column, as shown in Figure 3, stimulation of L1 gradually inhibited dendritic Ca^{2+} transients (top) and ADPs (bottom). Middle column, same protocol repeated in the presence of the $GABA_B$ antagonist CGP52432 (1 μM). Right column, same protocol repeated in the presence of both, CGP52432 and the $GABA_A$ antagonist gabazine (3 μM).

(B) Inhibition curves for ΔF/F values during glutamatergic blockade (red), in the presence of CGP52432 (blue), and in the presence of both CGP52432 and gabazine (green) in the experiment depicted in (A). Same colors apply to (C)–(E).

(C) Average ΔF/F inhibition curves (n = 11; mean ± SEM).

(D) Inhibition curves for ADP areas in the experiment depicted in (A).

(E) Average ADP inhibition curves (n = 11, mean ± SEM). Arrows indicate the drug-dependent shift of the inhibition curves. Dashed lines represent the values in the absence of L1 stimulation.

K^+ channels with Ba^{2+} increased the duration of the dendritic Ca^{2+} spike (Figure 6C) and decreased the critical frequency of APs that induced Ca^{2+} spikes. However, in the presence of Ba^{2+}, baclofen reduced the area under the Ca^{2+} spike by 4.7-fold more than in control conditions, indicating that $GABA_B$ inhibition of Ca^{2+} spikes was even more effective (Figure 6E). The enhanced effect of baclofen was probably due to the enhanced Ca^{2+} spike in comparison to control, but importantly Ba^{2+} never reduced the effect of puffing the $GABA_B$ agonist.

Could inhibition of Ca^{2+} currents underlie the blocking effect of baclofen? To further test this, we used dendritic voltage-clamp recordings in the Ca^{2+} initiation zone of the apical tuft (>500 μm; Figure 7A, inset) with a pipette containing an internal Cs^+-methanesulfonate based solution (see Experimental Procedures). Immediately after seal rupture, a current-voltage curve was performed (Figure 7A), and the presence of dendritic Ca^{2+} activity indicated the proximity of the recording site to the dendritic spike initiation zone (Amitai et al., 1993; Schiller et al., 1997).

The external medium was then supplemented with a "cocktail" for isolating Ca^{2+} currents containing the blockers TTX (1 μM), TEA (30 mM), and 4-AP (5 mM), and in three cells, Ba^{2+} (200 μM) was added. Because the results were the same with and without Ba^{2+}, we pooled the data. Under voltage clamp a series of voltage commands was injected into the dendrite (from −90 mV to 50 mV; holding voltage −80 mV). A family of inward currents was observed, followed by prolonged tail currents at the end of the voltage step (Figure 7B, black sweeps). The replacement of K^+ with Cs^+ in the internal solution and the use of an external solution containing Na^+ and K^+ channel blockers leave Ca^{2+} as the main source of ionic influx. Ca^{2+} currents were reversibly inhibited by the $GABA_B$ agonist baclofen (Figure 7C). The inward currents started developing a few milliseconds after the initiation of the voltage pulse possibly because of voltage escape of a nearby Ca^{2+} spike with inadequate space clamp of the dendritic segment. However, since the puffed baclofen was restricted to a small area (up to 100 μm; see Experimental Procedures), the inhibitory mechanism must have been close to the pipette situated in the Ca^{2+} spike initiation zone. Figure 7C depicts the temporal course of this inhibition. The inset on the left shows the experimental arrangement, whereas the inset on the right shows leak-subtracted Ca^{2+} currents recorded at the three different times indicated by the numbers 1–3 beside the curve. Identical results were observed in seven other dendritic recordings. Baclofen significantly reduced the integral

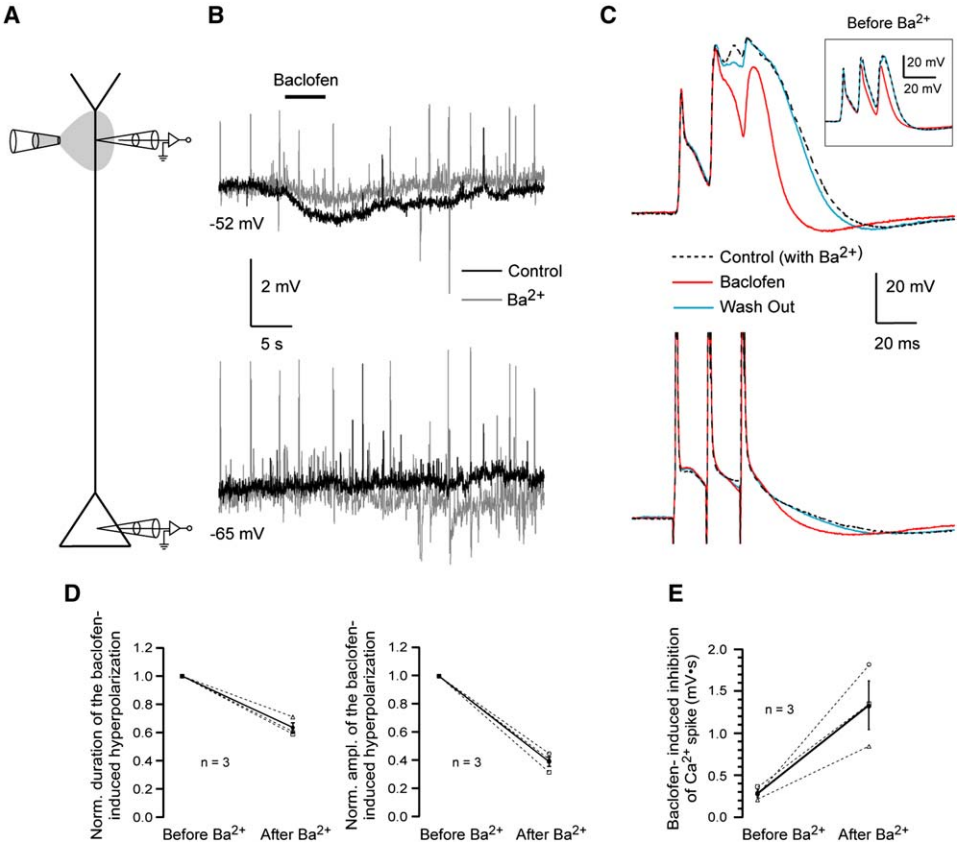

Figure 6. $GABA_B$-Induced Inhibition of Dendritic Ca^{2+} Spikes Is Not Reduced by Ba^{2+}

(A) Experimental configuration. Simultaneous somatic and distal (511 ± 40 μm from soma, n = 3) dendritic recordings were performed while a puffing pipette expelled baclofen (50 μM) onto the apical tuft.

(B) Recordings obtained from the apical tuft (top) and from the soma (bottom). Puffing baclofen onto the dendrite induced a locally restricted hyperpolarization that was not detected by the somatic recording (black sweeps). Ba^{2+} (200 μM) applied to the bath significantly diminished both, duration and amplitude of the hyperpolarization (gray sweeps, spontaneous APs observed in the presence of Ba^{2+} were truncated).

(C) Dendritic Ca^{2+} spikes (top) evoked with the CF protocol (dashed curves), before (inset) and after application of Ba^{2+}. Puffing baclofen on the dendritic tuft inhibited Ca^{2+} spikes (red sweeps) before and after application of Ba^{2+}. This inhibition was also reflected in the ADP (bottom).

(D) Summary of three recorded cells in which Ba^{2+} systematically reduced the duration (left) and amplitude (right) of the baclofen-induced hyperpolarization.

(E) Summary of the change in magnitude of the baclofen-induced inhibition of dendritic firing before and after Ba^{2+}. In (D) and (E), open symbols represent single experiments, and solid symbols represent the mean change (±SEM) before and after Ba^{2+}.

of the inward dendritic Ca^{2+} current by 64.5% ± 11% (n = 8; $p < 0.05$; Wilcoxon's test; Figure 7D). Puffing external solution without baclofen did not modify the Ca^{2+} currents (n = 2; data not shown). These results show that activation of $GABA_B$ receptors in the apical tuft directly inhibit Ca^{2+} conductances, which participate in dendritic firing.

Which $GABA_{B1}$ Isoform Mediates Long-Lasting Dendritic Inhibition?

It is becoming evident that the $GABA_{B1a}$ and $GABA_{B1b}$ isoforms mediate distinct physiological roles in the central nervous system (Vigot et al., 2006). Here, we examined whether an individual isoform is responsible for dendritic Ca^{2+} spike inhibition. There are no selective ligands for $GABA_{B1a}$ and $GABA_{B1b}$ available. We therefore used mice with a genetic lack of either isoform (Vigot et al., 2006). The intrinsic properties (i.e., resting V_m, input resistance, rheobase [AP current threshold], CF, and ADP values) of the neurons obtained from knockout mice were similar to wt ($p > 0.05$; Mann-Whitney U; Table 1).

Neurons from $GABA_{B1a}^{-/-}$ mice were not different to wt neurons and displayed both CGP52432- and gabazine-sensitive inhibitory components (n = 8, Figures 8A and 8B). In contrast, neurons from $GABA_{B1b}^{-/-}$ mice lacked the long-lasting inhibitory component, whereas stimulation of L1 was only effective in inhibiting Ca^{2+} spikes when applied <150 ms beforehand (n = 9, Figures 8C and 8D). This short-lasting inhibition was mediated by activation of $GABA_A$ receptors because it was abolished by gabazine. Somatically recorded ADPs showed the same results (data not shown).

To examine the location of the $GABA_{B1b}$ inhibition, we also compared the effect of puffing baclofen onto the soma and apical tufts of wt and knockout $GABA_B$ mice. Baclofen applied to the soma never affected dendritic firing in any of the animals tested (Figure 9). However, when puffed onto the dendrite, baclofen reversibly inhibited dendritic Ca^{2+} activity in both wt and $GABA_{B1a}^{-/-}$ but not in $GABA_{B1b}^{-/-}$ mice, as observed with direct dendritic recordings or by means of the somatic ADP (Figure 9D; wt ΔADP = 67.3 ± 12.6 mV · ms, n = 4;

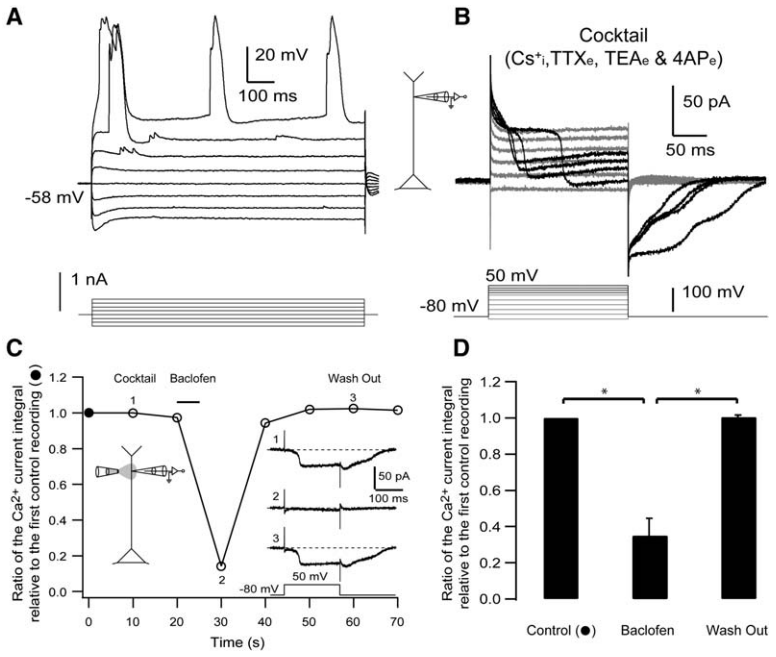

Figure 7. Activation of Dendritic $GABA_B$ Receptors Inhibits Dendritic Ca^{2+} Currents Directly

(A) Voltage recordings performed in current-clamp mode at a distal dendritic site (650 μm) immediately after seal rupture. Dendritic Ca^{2+} spikes occurred with depolarizing current steps (400 pA, 1000 ms duration).

(B) Depolarizing voltage commands (200 ms duration) in voltage-clamp mode were applied to the dendrite in an external medium containing TTX (1 μM), TEA (30 mM), and 4-AP (5 mM). Under these conditions, inward Ca^{2+} currents were recorded (black sweeps).

(C) Time course of inhibition of dendritic Ca^{2+} currents after a puff of external solution containing baclofen (50 μM; bar). Open circles represents the normalized integral of the inward Ca^{2+} current, as recorded during the voltage step, relative to the first control sweep (●). The interval between sweeps was 10 s. The agonist was ejected from a perfusion pipette placed 50 μm in front of the recording site. Representative Ca^{2+} currents (after leak subtraction) before (1), immediately after the agonist puff (2), and during washout (3) are shown in the right inset.

(D) Summary of the inhibitory effect of baclofen in eight dendritic recordings (mean ± SEM). Asterisk indicates significant differences in the normalized area underneath the inward Ca^{2+} current recordings.

$GABA_{B1a}^{-/-}$ ΔADP = 43 ± 1 mV · ms, n = 3; $GABA_{B1b}^{-/-}$ ΔADP = 0.09 ± 8.3 mV · ms, n = 3). Together, these results point to an exclusive role for dendritically located $GABA_{B1b}$ receptors in long-lasting inhibition of dendritic Ca^{2+} spikes.

Different Pre- and Postsynaptic Roles for $GABA_{B1a}$ and $GABA_{B1b}$

Activation of $GABA_B$ receptors on neocortical pyramidal neurons leads to the generation of slow K^+-mediated inhibitory postsynaptic potentials (Benardo, 1994; Gähwiler and Brown, 1985; Newberry and Nicoll, 1984; Shao and Burkhalter, 1999; Tamas et al., 2003). In slices obtained from wt mice, the compound IPSP evoked by L1 stimulation revealed a biphasic IPSP (Figure 10A, top, red trace) of 312.1 ± 15.2 ms duration (Figure 10C, wt, red bar; n = 16) as measured from the time of the first L1 shock to the time of return to baseline. For these experiments, we adjusted the stimulus intensity so that the resulting IPSP clearly had two components. This intensity was usually much stronger than necessary for blocking dendritic Ca^{2+} spikes. Under these conditions, CGP52432 abolished the slow component leaving an IPSP of 104.5 ± 12.2 ms duration (n = 16; $p < 0.05$; Wilcoxon's test; Figure 10C, wt, blue bar).

Interestingly, the $GABA_B$ antagonist significantly increased the amplitude of the fast IPSP component (Figure 10A, top, blue trace) by a 35% ± 6% ($p < 0.05$; Wilcoxon's test; Figure 10D). Disinhibition of presynaptic inhibitory terminals induced by CGP52432 could explain this observation. To test this, we performed a series of experiments (n = 5) in which we included GDP-β-S (1 mM) in the internal solution to disrupt the G protein-mediated postsynaptic signaling cascades. Immediately after cell rupture, L1 stimulation evoked a slow IPSP (data not shown). After 20 min loading the cells with GDP-β-S, the slow IPSP was inhibited and only the fast IPSP (108.9 ± 18 ms duration) was observed (Figure 10A, bottom, red trace). Under these conditions, CGP52432 did not affect the duration of the fast IPSP component (107.5 ± 14 ms; $p > 0.05$; Wilcoxon's test; Figure 10C) but did enhance its amplitude (Figure 10A, bottom, blue trace) by 54% ± 12% (n = 5; $p < 0.05$; Wilcoxon's test U; Figure 10D).

These experiments indicate that $GABA_B$ receptors acting presynaptically inhibit GABA release. In this scenario, CGP52432 results in more GABA being released and therefore a larger IPSP is observed. In addition, CGP52432 also uncovers a rebound potential observed at the end of the IPSP (see blue sweeps in Figures 10A and 10B), which may be due to the activation of conductances such as I_h. But which $GABA_B$ isoform accounts for the pre- versus postsynaptic modulation?

The slow CGP52432-sensitive postsynaptic IPSP was also observed in neurons from $GABA_{B1a}^{-/-}$ mice (Figure 10B, top, and Figure 10C; n = 9) but not in $GABA_{B1b}^{-/-}$ mice in which only a fast IPSP component (99.5 ± 26 ms duration) was present (Figure 10B; bottom) and whose duration was insensitive to CGP52432 (n = 12; $p > 0.05$; Wilcoxon's test; Figure 10C). The fast IPSP component observed in $GABA_{B1b}^{-/-}$ mice did not differ in duration to the fast IPSP seen in wild-type mice after the postsynaptic action of the G protein inhibitor, GDP-β-S (Figure 10C, $p > 0.05$; Mann-Whitney U).

The $GABA_B$ antagonist significantly increased the amplitude of the fast IPSP in $GABA_{B1b}^{-/-}$ mice (92% ± 16%; $p < 0.05$; Wilcoxon's test) but not in $GABA_{B1a}^{-/-}$ mice ($p > 0.05$; Wilcoxon's test; Figures 10B and 10D). In $GABA_{B1b}^{-/-}$ mice, the increase in amplitude of the fast IPSP was even bigger ($p < 0.05$; Mann-Whitney U)

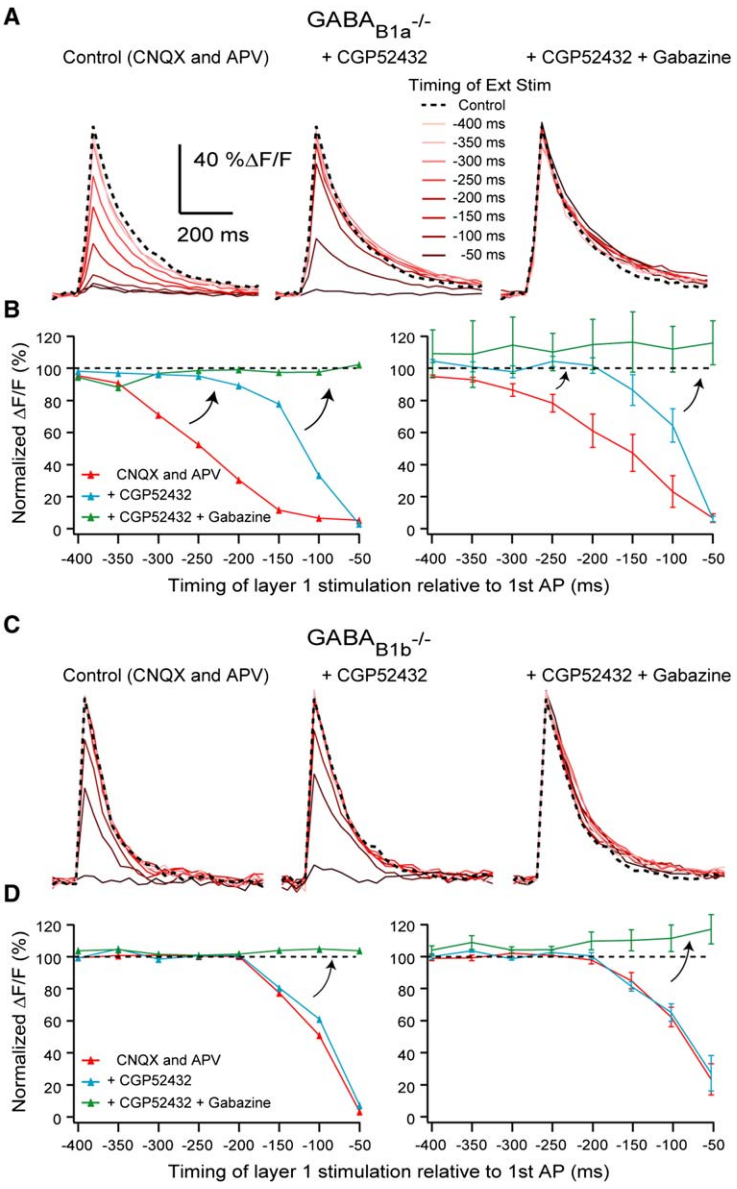

Figure 8. Genetic Lack of the $GABA_{B1b}$ but Not the $GABA_{B1a}$ Subunit Disrupts the Long-Lasting Inhibition of Dendritic Ca^{2+} Firing

(A) Same experimental procedure as in Figure 5 (for the sake of clarity, only the Ca^{2+} transients are shown), repeated in neurons from mice lacking the $GABA_{B1a}$-subunit isoform ($GABA_{B1a}^{-/-}$).

(B) Inhibition curves for the experiment shown in A (left) and the average inhibition curves for all experiments (n = 6; right; mean ± SEM).

(C) Same as (A) for mice lacking the $GABA_{B1b}$ subunit isoform ($GABA_{B1b}^{-/-}$).

(D) Same as (B) for $GABA_{B1b}^{-/-}$ mice (n = 7; mean ± SEM). Note, as in wt mice, inhibition curves for the $GABA_{B1a}$ show drug-dependent shifts (arrows) for both CGP52432 and gabazine, whereas $GABA_{B1b}$ inhibition curves were only gabazine sensitive.

than the one observed in wild-type, maybe indicating the existence of a compensatory mechanism in these mice. Interestingly, $GABA_{B1b}^{-/-}$ mice also responded to puff application of baclofen (Figure 9E), albeit smaller in amplitude and duration than the response in $GABA_{B1a}^{-/-}$ and wt mice (wt neurons: 29.5 s, −2.3 mV, n = 10; $GABA_{B1a}^{-/-}$: 46.1 s., −4.4 mV, n = 8; $GABA_{B1b}^{-/-}$: 20.2 s., −0.9 mV, n = 6). This result, which was also observed in hippocampal neurons lacking the $GABA_{B1b}$ isoform (Vigot et al., 2006), may reflect the expression of postsynaptic $GABA_{B1a}$ receptors at extrasynaptic locations. This may be due to compensatory mechanisms. Nevertheless, the fact that no block of Ca^{2+} spikes was observed in the $GABA_{B1b}^{-/-}$ mice despite the presence of a postsynaptic hyperpolarization and that no further block of Ca^{2+} spikes was observed with the additional hyperpolarization in $GABA_{B1a}^{-/-}$ mice suggests that the mechanism of dendritic inhibition described in this study is not correlated to the activation of GIRK channels.

Discussion

We have investigated the mechanisms by which inhibition blocks regenerative Ca^{2+} activity in the distal dendrites of layer 5 pyramidal neurons of the somatosensory cortex of both mice and rats. We found that dendritic Ca^{2+} activity can be blocked by inhibition that lasts up to 400 ms, suggesting that inhibition can modulate AP firing rate and firing mode for long periods. We found a shorter (<150 ms) inhibitory component dominated by the action of ionotropic $GABA_A$ receptors and a longer component (>150 ms) that was entirely due to postsynaptic metabotropic $GABA_B$ receptor activation, specifically involving the $GABA_{B1b}$ isoform and not the $GABA_{B1a}$ isoform, which mediates presynaptic inhibition of GABA release.

Previous studies in both hippocampal and neocortical L5 pyramidal neurons have shown inhibition of dendritic Ca^{2+} influx and associated burst firing in rats (Buzsaki

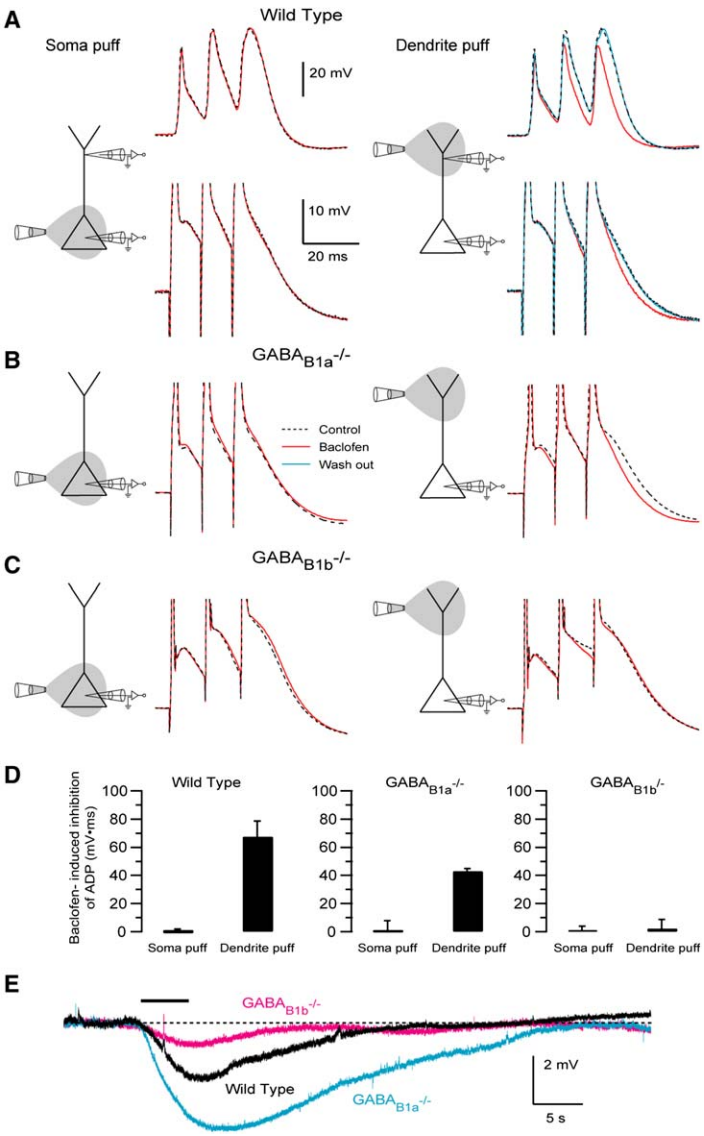

Figure 9. Activation of GABA$_{B1b}$ but Not GABA$_{B1a}$ Receptors in the Apical Tuft Only Inhibits Dendritic Ca^{2+} Spikes

(A) Experimental configuration. Simultaneous somatic and distal (>500 μm) dendritic recordings from a L5 pyramidal neuron in a wild-type mouse were performed while the GABA$_B$ agonist baclofen (50 μM) was sequentially puffed on the soma (first column) and then in the apical tuft (third column). Electrophysiological recordings obtained from each pipette are shown alongside. Dendritic Ca^{2+} spikes, evoked with the CF protocol (second and fourth columns, controls shown with dashed curves), were blocked when baclofen (red sweeps) was puffed onto the apical tuft but not when puffed near soma. The inhibitory action was washed out completely after ~40 s (blue sweeps in the fourth column).

(B and C) Same experimental procedures where performed for GABA$_{B1a}^{-/-}$ and GABA$_{B1b}^{-/-}$ neurons, although only somatic recordings were performed and dendritic activity was assessed with the ADP. Note that only GABA$_{B1b}^{-/-}$ mice lacked inhibitory responses when baclofen was puffed on the apical tuft.

(D) Summary of inhibitory effect of baclofen on the dendritic activity (mean ± SEM) when puffed on the soma and on the dendrite for wt (n = 4; left), GABA$_{B1a}^{-/-}$ (n = 3; middle), and GABA$_{B1b}^{-/-}$ mice (n = 3; right).

(E) Grand average of baclofen-induced hyperpolarizations when puffed and recorded from the soma of wt (n = 10, black sweep), GABA$_{B1a}^{-/-}$ (n = 8; blue sweep), and GABA$_{B1b}^{-/-}$ mice (n = 6; magenta sweep).

et al., 1996; Chen and Lambert, 1997; Kim et al., 1995; Larkum et al., 1999a, 1999b); however, a complete description of the timing and underlying mechanisms had not been carried out. Here, we observed that the identical timing and pharmacology of dendritic inhibition is preserved in both mice and rats, which highlights the importance of regulation of dendritic Ca^{2+} activity in cortical function in rodents.

The contribution and time course of GABA$_A$ and GABA$_B$ receptors in mediating dendritic inhibition are determined by their physiological actions, which are quite distinct. Upon activation, ionotropic GABA$_A$ receptors activate a chloride conductance, which can lead to a deflection in V_m and shunting inhibition. Which of these two mechanisms predominates in dendritic inhibition? A recent study suggests that the response of GABA$_A$ receptors might be depolarizing under physiological conditions and not hyperpolarizing as was previously assumed (Gulledge and Stuart, 2003). Regardless of the direction of V_m deflection, two lines of evidence suggest that the predominant effect of this conductance is mainly its shunting action: firstly, hyperpolarizing dendritic current injection did not block Ca^{2+} activity (data not shown); second, before the application of glutamatergic blockers, the compound EPSP/IPSP was depolarizing but was also effective in blocking dendritic Ca^{2+} activity (see also Staley and Mody [1992]). We therefore conclude that the major inhibitory influence of GABA$_A$ receptors is due to shunting inhibition and that their time of action is mainly limited by the kinetics of those receptors involved.

Understanding GABA$_B$-mediated inhibition is more complicated because of their activation of G protein-dependent signaling cascades with different targets (Bettler et al., 2004). Which targets underlie the long-lasting inhibition of dendritic Ca^{2+} spikes reported here? A small (~2–5 mV) long-lasting hyperpolarization was observed after L1 stimulation in the presence of glutamatergic blockers that could be abolished by the application of the GABA$_B$ blocker CGP52432 (Figure 10A). Direct application of the GABA$_B$ agonist baclofen also caused hyperpolarization postsynaptically (Figure 6 and Figure 9). This action is likely to be due to the activation of K^+ channels (Benardo, 1994; Gähwiler and Brown, 1985;

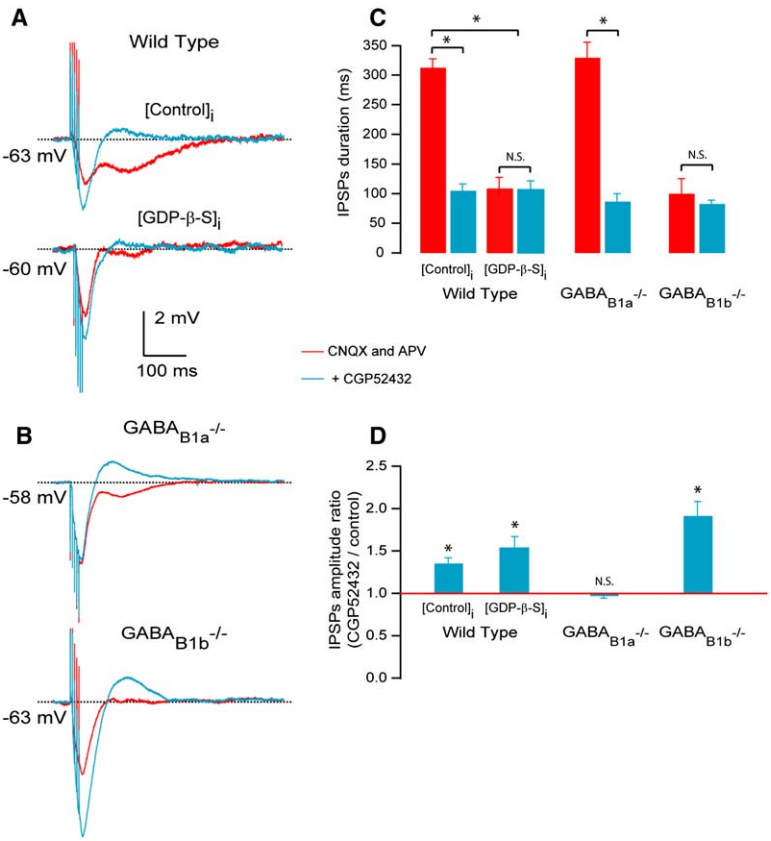

Figure 10. $GABA_{B1a}$ and $GABA_{B1b}$ Receptor Isoforms Exert Different Pre- and Postsynaptic Actions

(A) Top, stimulation of L1 in the presence of CNQX (10 μM) and APV (50 μM) induced a long-lasting biphasic IPSP (red trace) in L5 pyramidal neurons of wt mice. CGP52432 (1 μM) abolished the slow component of the IPSP but increased the amplitude of the remaining fast IPSP (blue trace); bottom, same recordings as before but with a pipette containing GDP-β-S (1 mM) that diffused into the postsynaptic neuron. After loading the cell for ~20 min, the slow IPSP component was inhibited, and the remaining fast component was observed (red trace). CGP52432 still increased the amplitude of the remaining IPSP.

(B) Same experimental configuration as in (A) but repeated in $GABA_{B1a}^{-/-}$ (top) and $GABA_{B1b}^{-/-}$ mice (bottom). The CGP52432-sensitive slow component was present in $GABA_{B1a}^{-/-}$ but not in $GABA_{B1b}^{-/-}$ mice. CGP52432 induced an increase in the amplitude of the remaining fast IPSP component only in $GABA_{B1b}^{-/-}$ mice.

(C) Average duration of the IPSP (mean ± SEM) in control conditions (red bars) and after application of CGP52432 (blue bars).

(D) Average CGP52432-induced increase in amplitude of the fast IPSP (mean ± SEM), normalized to control amplitudes (red line). For (C) and (D), an asterisk indicates a significant difference ($p < 0.05$), and "N.S." indicates no significant difference.

Newberry and Nicoll, 1984; Shao and Burkhalter, 1999; Tamas et al., 2003), which would introduce a shunt for the generation of dendritic Ca^{2+} spikes. On the other hand, IPSPs less than 100 ms in duration could inhibit Ca^{2+} spikes for up to 400 ms (e.g., Figure 1B). A robust inhibition of dendritic Ca^{2+} current could be induced by local application of the $GABA_B$ agonist, baclofen, even when K^+ currents were blocked, suggesting that the mechanism of inhibition via $GABA_B$ receptor activation relies mostly on the inhibition of Ca^{2+} channels with a smaller contribution because of shunt caused by K^+ channel activation.

It is not known which Ca^{2+} channels underlie the Ca^{2+} spike in the apical dendrite of layer 5 neocortical pyramidal neurons, although it is has been suggested that low-voltage activated T-type and high-voltage activated L- and N-type channels all exist, possibly in uniform density, along the apical dendrite (Migliore and Shepherd, 2002). Kavalali et al. (1997) showed that baclofen inhibits at least N-type and some other unspecified Ca^{2+} channels in hippocampal pyramidal dendrosomes. It is also unclear under which physiological conditions these Ca^{2+} channels are most likely to be activated. Dendritic Ca^{2+} spikes have been observed in vivo in L5 pyramidal neurons (Helmchen et al., 1999; Larkum and Zhu, 2002). Also, in vivo-like trains of APs have been shown to cause Ca^{2+} spikes in vitro (Williams and Stuart, 2000).

Postsynaptic versus Presynaptic $GABA_B$ Effects

The precise localization of $GABA_B$ receptors and the subunit isoforms from which they are composed is largely unknown (Bettler et al., 2004). Biochemical, in situ hybridization and immunohisotchemical studies have suggested that $GABA_{B1a}$ and $GABA_{B1b}$ are spatially segregated. However, because of the lack of selective pharmacological or biochemical tools, no consensus as to whether the isoforms are localized pre- or postsynaptically or both was reached (Benke et al., 1999; Bischoff et al., 1999; Fritschy et al., 1999; Liang et al., 2000; Poorkhalkali et al., 2000; Princivalle et al., 2001). Our data show that in the cortex, $GABA_{B1}$ isoforms subserve functionally different types of inhibition. In particular, $GABA_{B1b}$ receptors in the distal dendritic Ca^{2+} spike initiation zone of L5 pyramidal neurons selectively inhibit Ca^{2+} spikes while leaving spike propagation intact. The spatial segregation of $GABA_B$ isoforms may also prove crucial for the design of treatments for neurological and psychiatric disorders, in which $GABA_B$ receptors have been implicated (Bettler et al., 2004), in particular for diseases involving dendritic hyperexcitability such as epilepsy (Cossart et al., 2001; Schiller, 2004; Wong and Prince, 1979).

Sources of Inhibition

In the neocortex, about every fifth neuron and every sixth synaptic bouton synthesizes and releases GABA (Beaulieu et al., 1992; Beaulieu and Somogyi, 1990; Somogyi et al., 1998). Inhibitory interneurons have diverse morphologies, molecular and physiological properties, and selectively target different structures of pyramidal neurons (Markram et al., 2004; Somogyi et al., 1998). Inhibitory neurons innervating the tuft of pyramidal neurons may come from all layers (Markram et al., 2004; Somogyi et al., 1998), making it difficult to identify the

neuronal fingerprint of the inhibition reported here. The extracellular electrode was placed in L1 and the sources of inhibition are likely to be restricted to the same or nearby columns (Binzegger et al., 2004), although it may have come from any layer. The population of L1 interneurons is basically differentiated into two groups in adult rodents: multipolar cells, whose axons are vertically oriented extending into deeper cortical layers; and neurogliaform interneurons, whose axons extend horizontally in L1 contacting the apical tufts of pyramidal neurons (Chu et al., 2003; Hestrin and Armstrong, 1996).

The extracellular stimuli used in this study are likely to have also evoked APs in axons. Most of the inhibitory axons found in layer 1 of the somatosensory cortex are thought to come from somatostatin-immunoreactive cells whose cell bodies are actually in L2/3 (Shlosberg et al., 2003). Another source of $GABA_B$ activation could come from neurogliaform cells in L2/3 as a single AP of this neuron is able to evoke a long-lasting $GABA_B$-mediated IPSP in pyramidal neurons and other neurogliaform cells (Simon et al., 2005; Tamas et al., 2003). However, these IPSPs are highly depressing with a time constant of several tens of seconds, which argues against them playing a significant role in our experiments. $GABA_B$ receptors are also known to reside in extrasynaptic compartments (Fritschy et al., 1999) where they must be activated by spill over of GABA (Kim et al., 1997; Scanziani, 2000). This suggests that their activation would depend either on interneurons firing at high rates or many neurons acting synchronously (Scanziani, 2000). There are many candidate fast-spiking interneurons that are ubiquitously located in the cortex, although some (but not all) of these are ruled out because they target the persomatic region of pyramidal neurons (Markram et al., 2004; Somogyi et al., 1998). It is noteworthy that another contribution to the GABAergic synaptic contacts to distal apical dendrites of L5 pyramidal neurons comes from Martinotti cells from layers 2–6 (Thomson and Bannister, 2003; Wang et al., 2004), whose activity is tightly regulated by other L5 pyramidal neurons establishing a disynaptic inhibitory feedback loop (Silberberg et al., 2004, Soc. Neurosci., abstract).

The physiological conditions that lead to dendritic inhibition are as yet unknown, but the functional consequences of such inhibition are likely to be very important. L5 pyramidal neurons receive convergent excitatory inputs from L1 fibers which carry top-down information from higher cortical areas (Cauller et al., 1998; Felleman and Van Essen, 1991; Rockland and Pandya, 1979), feedback information from nonspecific thalamocortical pathways (Diamond, 1995), and feedback pathways from perirhinal and parahippocampal cortical areas (Lavenex and Amaral, 2000). These excitatory inputs have received a great deal of attention from many groups because of their possible influence on cognitive processes such an attention (Lamme et al., 1998; Olson et al., 2001) and binding of perceptual features (Cauller, 1995; Llinas et al., 2002).

The interaction of excitatory and inhibitory actions on the distal apical dendrite is undoubtedly a source of rich computational possibilities for the neocortex. For example, temporal coincidence of excitatory distal inputs with ongoing somatic spiking has been shown to evoke dendritic Ca^{2+} APs (Larkum et al., 1999b; Schaefer et al., 2003). This has been suggested as a mechanism by which cortical neurons associate feed-forward with feed-back information (Larkum et al., 1999b). The data shown here imply the existence of inhibitory mechanisms that specifically disrupt the linking factor in this interaction, the dendritic Ca^{2+} spike, while leaving normal spike initiation and propagation intact. This could have a powerful influence on cortical processes that may depend on the ability to link feed-forward and feed-back processes such as learning, attention, and binding.

Experimental Procedures

The generation of $GABA_{B1a}{}^{-/-}$ and $GABA_{B1b}{}^{-/-}$ mice is described in an accompanying article (Vigot et al., 2006). All experimental mice were male and kept in the BALB/c background. Animal handling was in strict accordance with the guidelines given by the veterinary office of the canton Bern-Switzerland.

In vitro electrophysiology and imaging were performed on L5 pyramidal neurons of the primary somatosensory cortex in parasagittal slices obtained from wild-type and mutant mice (P27–P35) and rats (P28–P56). After decapitation, the brain was rapidly removed into ice-cold, oxygenated solution containing (in mM): 125 NaCl, 25 $NaHCO_3$, 2.5 KCl, 1.25 NaH_2PO_4, 1 $MgCl_2$, 25 glucose, and 2 mM $CaCl_2$ (pH 7.4). Slices (300 μm thick) were cut with a vibrating microslicer and maintained at 37ºC in the above solution for 15–120 min before use. Slices were perfused continuously with the above solution at 35ºC ± 2ºC throughout the experiments. Whole-cell recordings from somata and from dendrites were obtained with the aid of infrared differential interference contrast optics or oblique illumination with Nikon Eclipse E600FN or Olympus BX51WI microscopes, respectively. Somatic (4–6 MΩ) and dendritic (10–20 MΩ) recording pipettes were filled with an intracellular solution containing (in mM): 135 K gluconate, 7 KCl, 10 HEPES, 10 Na_2-phosphocreatine, 4 Mg-ATP, 0.3 GTP, 0.2% biocytin (pH 7.2 with KOH), and 291–293 mOsm. In some experiments, the recording pipette included GDP-β-S (1 mM; Sigma-Aldrich) and in others with rats, 20–30 mM KCl and 110–120 K gluconate were used. The reversal potential for K^+ was calculated to be −107 mV and for Cl^- (−78 mV, −50 mV, and −40 mV for 7 mM, 20 mM, and 30 mM intracellular [Cl^-], respectively). The intracellular solution contained 10 μM Alexa 594 to aid in locating the dendrite. 100 μM Oregon green BAPTA-1 (OGB-1) was also added to the pipette solution for Ca^{2+} imaging (dyes from Molecular Probes, Eugene, OR). Inhibition was generated with a bipolar extracellular stimulating electrode (FHC, Maine) in the presence of CNQX and APV in the extracellular medium. The stimulating electrode was placed on the bottom half of layer 1, 100–200 μm from the apical tuft, and the position and stimulus strength adjusted until a response was observed postsynaptically. Extracellularly evoked stimuli could always block dendritic Ca^{2+} activity at some location and stimulus strength.

For isolated dendritic Ca^{2+} currents, internal solution consisted of (in mM): 108 Cs-Methanesulfonate, 9 HEPES, 14 Na_2-phosphocreatine, 4 Mg-ATP and 0.3 Na-GTP, 0.2% biocytin (pH 7.3) (with CsOH). External solution was as described before but included (in mM): 0.001 tetrodotoxin (TTX), 30 tetraethylammonium-chloride (TEA), and 5 4-aminopyridine AP (4-AP) (Sigma-Aldrich). Local perfusion of baclofen was achieved with an Eppendorf microinjector 5242 (Zeiss, Germany) and a somatic pipette. We calibrated the range of action of the puffing pipette by puffing TTX around the axon-hillock of a L5 pyramidal neuron when firing APs. The influence of TTX was within a 100 μm.

Electrophysiological recordings were obtained with Axoclamp-2B (Axon Instruments, Union City, CA) or Dagan BVC-700A amplifiers. Ca^{2+} imaging was performed by means of a frame transfer charge-coupled device camera (MicroMax, Roper Scientific, Tucson, AZ). The specimen was observed by epifluorecence with filter sets for FITC or Rhodamine fluorescence (Chroma Technolgy Corp.). Regions of interest (ROIs) were chosen online for averaging fluorescence transients. Fluorescence intensities were sampled at ~20–40 Hz. Fluorescence transients were expressed as fluorescence changes

after subtraction of the background trace and division by the resting fluorescence (%$\Delta F/F$) (Helmchen, 2005). Drugs were acquired from Tocris Cookson (Switzerland) and consisted of (in μM): 10 CNQX (6-cyano-7-nitroquioxaline-2,3-dione), 50 APV (DL-2-amino-5-phosphonopentanoic acid), 1 CGP52432, 3 gabazine (6-imino-3-[4-methoxyphenyl]-1[6H]-pyridazinebutanoic acid hydrobromide), and 50 baclofen.

Supplemental Data

The Supplemental Data for this article can be found online at http://www.neuron.org/cgi/content/full/50/4/603/DC1/.

Acknowledgments

We thank Drs. Gilad Silberberg and Hans R. Lüscher for their comments on the manuscript and D. Limoges and H. Rüchti for their expert technical support. This work was supported by the Swiss National Science Foundation (Grant Nr. PP00A-102721/1 to M.L., 3100-067100.01 to B.B.) and Novartis Pharma AG (B.B.).

Received: January 3, 2006
Revised: March 28, 2006
Accepted: April 12, 2006
Published: May 17, 2006

References

Amitai, Y., Friedman, A., Connors, B.W., and Gutnick, M.J. (1993). Regenerative activity in apical dendrites of pyramidal cells in neocortex. Cereb. Cortex *3*, 26–38.

Beaulieu, C., and Somogyi, P. (1990). Targets and quantitative distribution of GABAergic synapses in the visual cortex of the cat. Eur. J. Neurosci. *2*, 296–303.

Beaulieu, C., Kisvarday, Z., Somogyi, P., Cynader, M., and Cowey, A. (1992). Quantitative distribution of GABA-immunopositive and -immunonegative neurons and synapses in the monkey striate cortex (area 17). Cereb. Cortex *2*, 295–309.

Benardo, L.S. (1994). Separate activation of fast and slow inhibitory postsynaptic potentials in rat neocortex in vitro. J. Physiol. *476*, 203–215.

Benke, D., Honer, M., Michel, C., Bettler, B., and Mohler, H. (1999). gamma-aminobutyric acid type B receptor splice variant proteins GBR1a and GBR1b are both associated with GBR2 in situ and display differential regional and subcellular distribution. J. Biol. Chem. *274*, 27323–27330.

Bettler, B., Kaupmann, K., Mosbacher, J., and Gassmann, M. (2004). Molecular structure and physiological functions of GABA(B) receptors. Physiol. Rev. *84*, 835–867.

Binzegger, T., Douglas, R.J., and Martin, K.A. (2004). A quantitative map of the circuit of cat primary visual cortex. J. Neurosci. *24*, 8441–8453.

Bischoff, S., Leonhard, S., Reymann, N., Schuler, V., Shigemoto, R., Kaupmann, K., and Bettler, B. (1999). Spatial distribution of GABA(B)R1 receptor mRNA and binding sites in the rat brain. J. Comp. Neurol. *412*, 1–16.

Buzsaki, G., Penttonen, M., Nadasdy, Z., and Bragin, A. (1996). Pattern and inhibition-dependent invasion of pyramidal cell dendrites by fast spikes in the hippocampus in vivo. Proc. Natl. Acad. Sci. USA *93*, 9921–9925.

Campbell, V., Berrow, N., and Dolphin, A.C. (1993). GABAB receptor modulation of Ca^{2+} currents in rat sensory neurones by the G protein G(0): antisense oligonucleotide studies. J. Physiol. *470*, 1–11.

Cauller, L. (1995). Layer I of primary sensory neocortex: where top-down converges upon bottom-up. Behav. Brain Res. *71*, 163–170.

Cauller, L.J., Clancy, B., and Connors, B.W. (1998). Backward cortical projections to primary somatosensory cortex in rats extend long horizontal axons in layer I. J. Comp. Neurol. *390*, 297–310.

Chen, H., and Lambert, N.A. (1997). Inhibition of dendritic calcium influx by activation of G-protein-coupled receptors in the hippocampus. J. Neurophysiol. *78*, 3484–3488.

Chu, Z., Galarreta, M., and Hestrin, S. (2003). Synaptic interactions of late-spiking neocortical neurons in layer 1. J. Neurosci. *23*, 96–102.

Cossart, R., Dinocourt, C., Hirsch, J.C., Merchan-Perez, A., De Felipe, J., Ben Ari, Y., Esclapez, M., and Bernard, C. (2001). Dendritic but not somatic GABAergic inhibition is decreased in experimental epilepsy. Nat. Neurosci. *4*, 52–62.

Costa, E., Auta, J., Grayson, D.R., Matsumoto, K., Pappas, G.D., Zhang, X., and Guidotti, A. (2002). GABAA receptors and benzodiazepines: a role for dendritic resident subunit mRNAs. Neuropharmacology *43*, 925–937.

de Blas, A.L., Vitorica, J., and Friedrich, P. (1988). Localization of the GABAA receptor in the rat brain with a monoclonal antibody to the 57,000 Mr peptide of the GABAA receptor/benzodiazepine receptor/Cl- channel complex. J. Neurosci. *8*, 602–614.

DeFelipe, J., and Jones, E.G. (1988). Cajal on the cerebral cortex: an annotated translation of the complete writings (Oxford, UK: Oxford University Press).

Derer, P., and Derer, M. (1990). Cajal-Retzius cell ontogenesis and death in mouse brain visualized with horseradish peroxidase and electron microscopy. Neuroscience *36*, 839–856.

Diamond, M.E. (1995). Somatosensory thalamus of the rat. In Cerebral Cortex: The Barrel Cortex of Rodents, E.G. Jones and M.E. Diamond, eds. (New York, NY: Plenum), pp. 189–220.

Felleman, D.J., and Van Essen, D.C. (1991). Distributed hierarchical processing in the primate cerebral cortex. Cereb. Cortex *1*, 1–47.

Fritschy, J.M., Weinmann, O., Wenzel, A., and Benke, D. (1998). Synapse-specific localization of NMDA and GABA(A) receptor subunits revealed by antigen-retrieval immunohistochemistry. J. Comp. Neurol. *390*, 194–210.

Fritschy, J.M., Meskenaite, V., Weinmann, O., Honer, M., Benke, D., and Mohler, H. (1999). GABAB-receptor splice variants GB1a and GB1b in rat brain: developmental regulation, cellular distribution and extrasynaptic localization. Eur. J. Neurosci. *11*, 761–768.

Gähwiler, B.H., and Brown, D.A. (1985). GABAb-receptor-activated K+ current in voltage-clamped CA3 pyramidal cells in hippocampal cultures. Proc. Natl. Acad. Sci. USA *82*, 1558–1562.

Gonchar, Y., and Burkhalter, A. (1997). Three distinct families of GABAergic neurons in rat visual cortex. Cereb. Cortex *7*, 347–358.

Gonchar, Y., and Burkhalter, A. (1999). Differential subcellular localization of forward and feedback interareal inputs to parvalbumin expressing GABAergic neurons in rat visual cortex. J. Comp. Neurol. *406*, 346–360.

Gonchar, Y., and Burkhalter, A. (2003). Distinct GABAergic targets of feedforward and feedback connections between lower and higher areas of rat visual cortex. J. Neurosci. *23*, 10904–10912.

Gonchar, Y., Pang, L.Y., Malitschek, B., Bettler, B., and Burkhalter, A. (2001). Subcellular localization of GABA(B) receptor subunits in rat visual cortex. J. Comp. Neurol. *431*, 182–197.

Gulledge, A.T., and Stuart, G.J. (2003). Excitatory actions of GABA in the cortex. Neuron *37*, 299–309.

Helmchen, F. (2005). Calibration of fluorescent calcium indicators. In Imaging Neurons: A Laboratory Manual, R. Yuste and A. Konnerth, eds. (New York: Cold Spring Harbor Laboratory), pp. 253–263.

Helmchen, F., Svoboda, K., Denk, W., and Tank, D.W. (1999). In vivo dendritic calcium dynamics in deep-layer cortical pyramidal neurons. Nat. Neurosci. *2*, 989–996.

Hestrin, S., and Armstrong, W.E. (1996). Morphology and physiology of cortical neurons in layer I. J. Neurosci. *16*, 5290–5300.

Houser, C.R., Hendry, S.H., Jones, E.G., and Vaughn, J.E. (1983). Morphological diversity of immunocytochemically identified GABA neurons in the monkey sensory-motor cortex. J. Neurocytol. *12*, 617–638.

Kavalali, E.T., Zhuo, M., Bito, H., and Tsien, R.W. (1997). Dendritic Ca^{2+} channels characterized by recordings from isolated hippocampal dendritic segments. Neuron *18*, 651–663.

Kim, H.G., Beierlein, M., and Connors, B.W. (1995). Inhibitory control of excitable dendrites in neocortex. J. Neurophysiol. *74*, 1810–1814.

Kim, U., Sanchez-Vives, M.V., and McCormick, D.A. (1997). Functional dynamics of GABAergic inhibition in the thalamus. Science *278*, 130–134.

Lamme, V.A.F., Super, H., and Spekreijse, H. (1998). Feedforward, horizontal, and feedback processing in the visual cortex. Curr. Opin. Neurobiol. *8*, 529–535.

Larkum, M.E., and Zhu, J.J. (2002). Signaling of layer 1 and whisker-evoked Ca^{2+} and Na^{+} action potentials in distal and terminal dendrites of rat neocortical pyramidal neurons in vitro and in vivo. J. Neurosci. *22*, 6991–7005.

Larkum, M.E., Kaiser, K.M., and Sakmann, B. (1999a). Calcium electrogenesis in distal apical dendrites of layer 5 pyramidal cells at a critical frequency of back-propagating action potentials. Proc. Natl. Acad. Sci. USA *96*, 14600–14604.

Larkum, M.E., Zhu, J.J., and Sakmann, B. (1999b). A new cellular mechanism for coupling inputs arriving at different cortical layers. Nature *398*, 338–341.

Lavenex, P., and Amaral, D.G. (2000). Hippocampal-neocortical interaction: a hierarchy of associativity. Hippocampus *10*, 420–430.

Liang, F., Hatanaka, Y., Saito, H., Yamamori, T., and Hashikawa, T. (2000). Differential expression of gamma-aminobutyric acid type B receptor-1a and -1b mRNA variants in GABA and non-GABAergic neurons of the rat brain. J. Comp. Neurol. *416*, 475–495.

Llinas, R.R., Leznik, E., and Urbano, F.J. (2002). Temporal binding via cortical coincidence detection of specific and nonspecific thalamocortical inputs: a voltage-dependent dye-imaging study in mouse brain slices. Proc. Natl. Acad. Sci. USA *99*, 449–454.

López-Bendito, G., Shigemoto, R., Kulik, A., Paulsen, O., Fairen, A., and Lujan, R. (2002). Expression and distribution of metabotropic GABA receptor subtypes GABABR1 and GABABR2 during rat neocortical development. Eur. J. Neurosci. *15*, 1766–1778.

Markram, H., Toledo-Rodriguez, M., Wang, Y., Gupta, A., Silberberg, G., and Wu, C. (2004). Interneurons of the neocortical inhibitory system. Nat. Rev. Neurosci. *5*, 793–807.

Migliore, M., and Shepherd, G.M. (2002). Emerging rules for the distributions of active dendritic conductances. Nat. Rev. Neurosci. *3*, 362–370.

Miles, R., Toth, K., Gulyas, A.I., Hajos, N., and Freund, T.F. (1996). Differences between somatic and dendritic inhibition in the hippocampus. Neuron *16*, 815–823.

Mintz, I.M., and Bean, B.P. (1993). GABAB receptor inhibition of P-type Ca^{2+} channels in central neurons. Neuron *10*, 889–898.

Newberry, N.R., and Nicoll, R.A. (1984). Direct hyperpolarizing action of baclofen on hippocampal pyramidal cells. Nature *308*, 450–452.

Olson, I.R., Chun, M.M., and Allison, T. (2001). Contextual guidance of attention: human intracranial event-related potential evidence for feedback modulation in anatomically early, temporally late stages of visual processing. Brain *124*, 1417–1425.

Poorkhalkali, N., Juneblad, K., Jonsson, A.C., Lindberg, M., Karlsson, O., Wallbrandt, P., Ekstrand, J., and Lehmann, A. (2000). Immunocytochemical distribution of the GABA(B) receptor splice variants GABA(B) R1a and R1b in the rat CNS and dorsal root ganglia. Anat. Embryol. (Berl.) *201*, 1–13.

Princivalle, A.P., Pangalos, M.N., Bowery, N.G., and Spreafico, R. (2001). Distribution of GABA(B(1a)), GABA(B(1b)) and GABA(B2) receptor protein in cerebral cortex and thalamus of adult rats. Neuroreport *12*, 591–595.

Radnikow, G., Feldmeyer, D., and Lubke, J. (2002). Axonal projection, input and output synapses, and synaptic physiology of Cajal-Retzius cells in the developing rat neocortex. J. Neurosci. *22*, 6908–6919.

Rockland, K.S., and Pandya, D.N. (1979). Laminar origins and terminations of cortical connections of the occipital lobe in the rhesus-monkey. Brain Res. *179*, 3–20.

Scanziani, M. (2000). GABA spillover activates postsynaptic GABA(B) receptors to control rhythmic hippocampal activity. Neuron *25*, 673–681.

Schaefer, A.T., Larkum, M.E., Sakmann, B., and Roth, A. (2003). Coincidence detection in pyramidal neurons is tuned by their dendritic branching pattern. J. Neurophysiol. *89*, 3143–3154.

Schiller, J., Schiller, Y., Stuart, G., and Sakmann, B. (1997). Calcium action potentials restricted to distal apical dendrites of rat neocortical pyramidal neurons. J. Physiol. *505*, 605–616.

Schiller, Y. (2004). Activation of a calcium-activated cation current during epileptiform discharges and its possible role in sustaining seizure-like events in neocortical slices. J. Neurophysiol. *92*, 862–872.

Scholz, K.P., and Miller, R.J. (1991). GABAB receptor-mediated inhibition of Ca^{2+} currents and synaptic transmission in cultured rat hippocampal neurones. J. Physiol. *444*, 669–686.

Shao, Z.W., and Burkhalter, A. (1999). Role of GABA(B) receptor-mediated inhibition in reciprocal interareal pathways of rat visual cortex. J. Neurophysiol. *81*, 1014–1024.

Shlosberg, D., Patrick, S.L., Buskila, Y., and Amitai, Y. (2003). Inhibitory effect of mouse neocortex layer I on the underlying cellular network. Eur. J. Neurosci. *18*, 2751–2759.

Simon, A., Olah, S., Molnar, G., Szabadics, J., and Tamas, G. (2005). Gap-junctional coupling between neurogliaform cells and various interneuron types in the neocortex. J. Neurosci. *25*, 6278–6285.

Somogyi, P., Tamas, G., Lujan, R., and Buhl, E.H. (1998). Salient features of synaptic organisation in the cerebral cortex. Brain Res. Brain Res. Rev. *26*, 113–135.

Staley, K.J., and Mody, I. (1992). Shunting of excitatory input to dentate gyrus granule cells by a depolarizing GABAA receptor-mediated postsynaptic conductance. J. Neurophysiol. *68*, 197–212.

Stuart, G., and Spruston, N. (1998). Determinants of voltage attenuation in neocortical pyramidal neuron dendrites. J. Neurosci. *18*, 3501–3510.

Stuart, G., Spruston, N., Sakmann, B., and Häusser, M. (1997). Action potential initiation and backpropagation in neurons of the mammalian CNS. Trends Neurosci. *20*, 125–131.

Takigawa, T., and Alzheimer, C. (1999). G protein-activated inwardly rectifying K^{+} (GIRK) currents in dendrites of rat neocortical pyramidal cells. J. Physiol. *517*, 385–390.

Tamas, G., Lorincz, A., Simon, A., and Szabadics, J. (2003). Identified sources and targets of slow inhibition in the neocortex. Science *299*, 1902–1905.

Thomson, A.M., and Bannister, A.P. (2003). Interlaminar connections in the neocortex. Cereb. Cortex *13*, 5–14.

Tsubokawa, H., and Ross, W.N. (1996). IPSPs modulate spike backpropagation and associated $[Ca^{2+}]i$ changes in the dendrites of hippocampal CA1 pyramidal neurons. J. Neurophysiol. *76*, 2896–2906.

Vigot, R., Barbieri, S., Bräuner-Osborne, H., Turecek, R., Shigemoto, R., Zhang, Y.-P., Luján, R., Jacobson, L.H., Biermann, B., Fritschy, J.-M., et al. (2006). Differential compartmentalization and distinct functions of $GABA_B$ receptor variants. Neuron *50*, this issue, 589–601.

Wang, Y., Toledo-Rodriguez, M., Gupta, A., Wu, C., Silberberg, G., Luo, J., and Markram, H. (2004). Anatomical, physiological and molecular properties of Martinotti cells in the somatosensory cortex of the juvenile rat. J. Physiol. *561*, 65–90.

Williams, S.R. (2005). Encoding and decoding of dendritic excitation during active states in pyramidal neurons. J. Neurosci. *25*, 5894–5902.

Williams, S.R., and Stuart, G.J. (2000). Backpropagation of physiological spike trains in neocortical pyramidal neurons: implications for temporal coding in dendrites. J. Neurosci. *20*, 8238–8246.

Wong, R.K., and Prince, D.A. (1979). Dendritic mechanisms underlying penicillin-induced epileptiform activity. Science *204*, 1228–1231.

Zhu, Y., Stornetta, R.L., and Zhu, J.J. (2004). Chandelier cells control excessive cortical excitation: characteristics of whisker-evoked synaptic responses of layer 2/3 nonpyramidal and pyramidal neurons. J. Neurosci. *24*, 5101–5108.